

**STUDY ON STRUCTURAL AND MAGNETIC PROPERTIES OF**  
 **$\text{Mn}_{(1-x)}\text{Zn}_x\text{Fe}_2\text{O}_4$  PREPARED BY SOLID-STATE REACTION METHOD**

A THESIS SUBMITTED IN PARTIAL FULFILLMENT  
OF THE REQUIREMENTS FOR THE DEGREE OF

**BACHELOR OF TECHNOLOGY**  
**IN CERAMIC ENGINEERING**

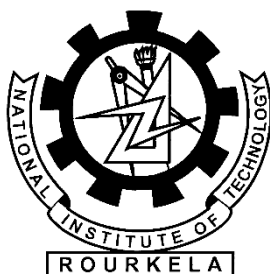
BY

**BIKASH BADAIAK**

111CR0550

Under the guidance of

**Prof. Arun Chowdhury**



**DEPARTMENT OF CERAMIC ENGINEERING**  
**NATIONAL INSTITUTE OF TECHNOLOGY**  
**ROURKELA – 769008**

**2014-15**



**National Institute of Technology, Rourkela**

**CERTIFICATE**

---

This is to certify that the thesis entitled “Study on Structural and Magnetic properties of  $\text{Mn}_{(1-x)}\text{Zn}_x\text{Fe}_2\text{O}_4$  prepared by solid-state reaction method” submitted by Bikash Badaik (Roll No. 111CR0550) in partial fulfilment of the requirements for the award of Bachelor of Technology degree in Ceramic Engineering at the National Institute of Technology, Rourkela is an authentic work carried out by him under my supervision and guidance.

To the best of my knowledge, the matter embodied in this thesis has not formed the basis for the award of any Degree or Diploma or similar title of any University or Institution.

**Date:**

**Arun Choudhury**  
**Assistant Professor**  
**Ceramic Engineering Department**  
**NIT, Rourkela-769008**

## ACKNOWLEDGEMENT

---

I would like to express my profound gratitude and indebtedness to Prof. Arun Chowdhury, Ceramic Engineering Department, NIT Rourkela for his guidance and valuable suggestions. This work would not have been possible without his encouragement and constructive criticism. I sincerely thank him for the time and patience he devoted for this work.

I am also thankful to all the faculty members for their valuable suggestions.

I am immensely thankful to Mr. Arvind Kumar and Mr. Bapi da for their help in carrying out the laboratory experiments.

I would like to acknowledge the authors of different research paper referred in the work, which were a valuable source for understanding the subject.

Lastly, I am thankful to all my friends who encouraged and helped me in accomplishing this project.

**Bikash Badaik**  
111CR0550  
Department of Ceramic Engineering  
NIT Rourkela

# CONTENTS

<b><u>Serial No.</u></b>	<b>Description</b>	<b>Page No.</b>
<b>I.</b>	<b>CERTIFICATE</b>	<b>1</b>
<b>II.</b>	<b>ACKNOWLEDGEMENT</b>	<b>2</b>
<b>III.</b>	<b>LIST OF FIGURES</b>	<b>4</b>
<b>IV.</b>	<b>LIST OF TABLES</b>	<b>5</b>
<b>V.</b>	<b>ABSTRACT</b>	<b>7</b>
<b>1.</b>	<b>INTRODUCTION</b>	<b>8</b>
<b>2.</b>	<b>LITERATURE REVIEW AND OBJECTIVE</b>	<b>11</b>
<b>3.</b>	<b>EXPERIMENTAL PROCEDURE</b>	<b>15</b>
<b>3.2</b>	<b>SOLID OXIDE MIXING METHOD</b>	<b>16</b>
<b>3.2.1</b>	<b>MIXING</b>	<b>16</b>
<b>3.2.2</b>	<b>CALCINATION</b>	<b>17</b>
<b>3.2.3</b>	<b>SAMPLE PRPARATIONAND EXPERIMENTATION OF POWDER XRD.</b>	<b>17</b>
<b>3.2.4</b>	<b>FORMING</b>	<b>17</b>
<b>3.2.5</b>	<b>SINTERING</b>	<b>18</b>
<b>3.3</b>	<b>CHARACTERIZATION</b>	<b>20</b>
<b>3.3.1</b>	<b>PHASE ANALYSIS BY XRD</b>	<b>20</b>
<b>3.3.2</b>	<b>APPARENT POROSITY AND BULK DENSITY</b>	<b>20</b>
<b>3.3.3</b>	<b>MICROSTRUCTURE ANALYSIS</b>	<b>21</b>
<b>3.3.4</b>	<b>B-H LOOP MEASUREMENT</b>	<b>21</b>
<b>4</b>	<b>RESULTS AND DISCUSSION</b>	<b>22</b>
<b>4.1</b>	<b>X-RAY DIFFRACTION ANALYSIS AND CRYSTALLITE SIZE</b>	<b>23</b>

4.2	<b>MICROSTRUCTURAL CHARACTERIZATION</b>	29
4.3	<b>BULK DENSITY</b>	32
4.4	<b>MAGNETIC CHARACTERIZATION</b>	34
5	<b>CONCLUSION</b>	36
	<b>REFERENCES</b>	38

### List of Figures

<b>Sl. No.</b>	<b>Figure</b>	<b>Page No.</b>
1.	Unit cell of Mn-Zn Ferrite	10
2.	B-H loop of Mn Zn Fe <sub>2</sub> O <sub>4</sub>	13
3.	Flow chart for the synthesis of Manganese Zinc Ferrite.	19
4.	XRD pattern of calcined powder (1000 °C/2hr) Mn <sub>(1-x)</sub> Zn <sub>x</sub> Fe <sub>2</sub> O <sub>4</sub> ; x = 0.1,0.2 and 0.3	23
5.	XRD pattern of sintered Mn <sub>(1-x)</sub> Zn <sub>x</sub> ferrite pellets at 1225 <sup>0</sup> C ,(x=0.1,0.2,0.3)	25
6.	XRD plot of Mn-ZnFe <sub>2</sub> O <sub>4</sub> pellets of 0.1 ,0.2 0.3 composition respectively sintered at 1250 °C for 2hr	26
7.	XRD plot of Mn-ZnFe <sub>2</sub> O <sub>4</sub> pellets of 0.1 ,0.2 0.3 composition respectively sintered at 1275 <sup>0</sup> C for 2hr	27
8.	XRD plot of Mn-Zn Fe <sub>2</sub> O <sub>4</sub> pellets of 0.1 ,0.2 0.3 composition respectively sintered at 1300 °C for 4hr	28
9.	Microstructrures of compositions of Mn <sub>(1-x)</sub> Zn <sub>x</sub> Fe <sub>2</sub> O <sub>4</sub> sintered at 1250 <sup>0</sup> C for 2hr	29
10.	Microstructrures of composition of Mn <sub>(1-x)</sub> Zn <sub>x</sub> Fe <sub>2</sub> O <sub>4</sub> sintered at 1275 <sup>0</sup> C for 2 hr	30

<b>11.</b>	<b>Microstructures of composition of <math>Mn_{(1-x)}Zn_xFe_2O_4</math> sintered at 1300°C for 4 hrs</b>	<b>31</b>
<b>12.</b>	<b>B-H loop of <math>Mn Zn Fe_2O_4</math> sintered at 1300°C for 4 hours having 0.3 Zn</b>	<b>34</b>

### List of Tables

<b>Sl. No.</b>	<b>Table No.</b>	<b>Page No.</b>
<b>1.</b>	<b>Amount of different composition taken in grams.</b>	<b>16</b>
<b>2.</b>	<b>Firing schedule and sintering temperatures.</b>	<b>18</b>
<b>3.</b>	<b>Crystallite Size of calcined <math>Mn_{(1-x)}Zn_xFe_2O_4</math> powders at 1000 °C, (x= 0.1, 0.2 0.3)</b>	<b>24</b>
<b>4.</b>	<b>lattice parameter and crystallite size of calcined ferrites <math>Mn_{0.9}Zn_{0.1}Fe_2O_4</math>, <math>Mn_{0.8}Zn_{0.2}Fe_2O_4</math> and <math>Mn_{0.7}Zn_{0.3}Fe_2O_4</math> at 1225 °C for 2hr</b>	<b>25</b>
<b>5.</b>	<b>lattice parameter and crystallite size of calcined ferrites <math>Mn_{0.9}Zn_{0.1}Fe_2O_4</math>, <math>Mn_{0.8}Zn_{0.2}Fe_2O_4</math> and <math>Mn_{0.7}Zn_{0.3}Fe_2O_4</math> at 1250 °C for 2hr</b>	<b>26</b>
<b>6.</b>	<b>lattice parameter and crystallite size of calcined ferrites <math>Mn_{0.9}Zn_{0.1}Fe_2O_4</math>, <math>Mn_{0.8}Zn_{0.2}Fe_2O_4</math> and <math>Mn_{0.7}Zn_{0.3}Fe_2O_4</math> at 1275 °C for 2hr</b>	<b>27</b>
<b>7.</b>	<b>lattice parameter and crystallite size of calcined ferrites <math>Mn_{0.9}Zn_{0.1}Fe_2O_4</math>, <math>Mn_{0.8}Zn_{0.2}Fe_2O_4</math> and <math>Mn_{0.7}Zn_{0.3}Fe_2O_4</math> at 1300 °C for 4hr</b>	<b>28</b>
<b>8.</b>	<b>Average grain size of compositions sintered at 1250°C for 2 hours</b>	<b>30</b>
<b>9.</b>	<b>Average grain size of compositions sintered at 1275°C for 2 hours</b>	<b>31</b>
<b>10.</b>	<b>Average grain sizes of larger, medium and smaller grain.</b>	<b>32</b>

<b>11.</b>	<b>B.D. and A.P of <math>Mn_{(1-x)} Zn_x Fe_2O_4</math> sintered at 1225 °C for 2 hour</b>	<b>32</b>
<b>12.</b>	<b>B.D. and A.P of <math>Mn_{(1-x)} Zn_x Fe_2O_4</math> sintered at 1250 °C for 2 hour</b>	<b>33</b>
<b>13.</b>	<b>B.D. and A.P of <math>Mn_{(1-x)} Zn_x Fe_2O_4</math> sintered at 1275 °C for 2 hour</b>	<b>33</b>
<b>14.</b>	<b>B.D. and A.P of <math>Mn_{(1-x)} Zn_x Fe_2O_4</math> sintered at 1300 °C for 2 hour</b>	<b>33</b>
<b>15.</b>	<b>Magnetic order parameters of <math>Mn_{(1-x)} Zn_x Fe_2O_4</math> sintered at 1275 °C/2hr</b>	<b>35</b>

## ABSTRACT

Reagent graded raw materials were used as starting material to synthesize and get characterization of Manganese-Zinc based spinel ferrite. Conventional solid-state reaction procedure was employed to produce specimens of  $\text{Mn}_{(1-x)}\text{Zn}_x\text{Fe}_2\text{O}_4$ , where  $x = 0.1, 0.2$  and  $0.3$ . The following study of Mn-Zn ferrite is done by solid oxidising method by varying Zn composition from 0.1 weight% to 0.3 weight% at temperatures  $1225^\circ\text{C}$ ,  $1250^\circ\text{C}$ , and  $1275^\circ\text{C}$ . X-ray diffraction analysis was done to report phases evolved with corresponding temperature. Scanning electron microscopy with a Field-Emission-SEM was employed to characterize microscopy images of ferrites samples. Bulk density, apparent porosity, crystallite size, average grain size, indexing were done. And regarding magnetic properties, B-H loop, saturation magnetization, coercivity, and residual magnetization were also done. It was observed that on increasing the composition of Zn and the temperature, the density increased. At the temperature  $1275^\circ\text{C}$  highest density is achieved. The average grain size also increased gradually. The saturation magnetization got improved. The residual magnetization value was good. The coercivity value decreased gradually on increasing both the composition of Zn and the temperature.


**Bikash Badaik**

111CR0550

Department of Ceramic Engineering  
NIT Rourkela



# **CHAPTER 1**



## **I INTRODUCTION**

## INTRODUCTION:

Mn–Zn ferrites are very important soft magnetic materials because of their high initial magnetic permeability, saturation magnetization, electrical resistivity and low power losses. These materials are extensively used as inductors, transformers, antenna rods, loading coils, deflection yokes, choke coils, recording heads, magnetic amplifiers, electromagnetic interference devices (EMI), power transformers and splitters. Moreover, Mn–Zn ferrites are very important in biomedicine as magnetic carriers for bio-separation, enzymes and proteins immobilization.

Ferromagnetic materials are magnetic ceramics which are used for making many devices such as permanent magnets, memory storing devices, and microwave machines and for the telecommunication machines purpose. Spinel ferrites have been researched for their magnetic and electrical properties. Among all, zinc manganese ferrite ( $\text{Mn}_{(1-x)}\text{Zn}_x\text{Fe}_2\text{O}_4$ ) possesses excellent properties including high magnetic permeability, saturation magnetization, and electrical resistivity, as well as low power loss at high frequencies. Magnetic spinels have the general formula  $\text{MO} \cdot \text{Fe}_2\text{O}_3$  or  $\text{MFe}_2\text{O}_4$  where, M is divalent metal ion like Mn, Zn, Ni, Fe, or Co (or a mixture of such ions). In the spinel crystal structure the oxygen ions form a cubic close-packed array in which two types of interstice occur, one coordinated tetrahedrally and the other octahedrally with oxygen ions. The unit cell shown in Fig 1 is seen to be made up of octants, four containing one type of structure (shaded) and four containing another (unshaded). In this representation some of the A-site cations lie at the corners and face-centre positions of the large cube; a tetrahedral and an octahedral site are shown. The close-packed layers of the oxygen ion lattice lie at right angles to the body diagonals of the cube.[1,2]

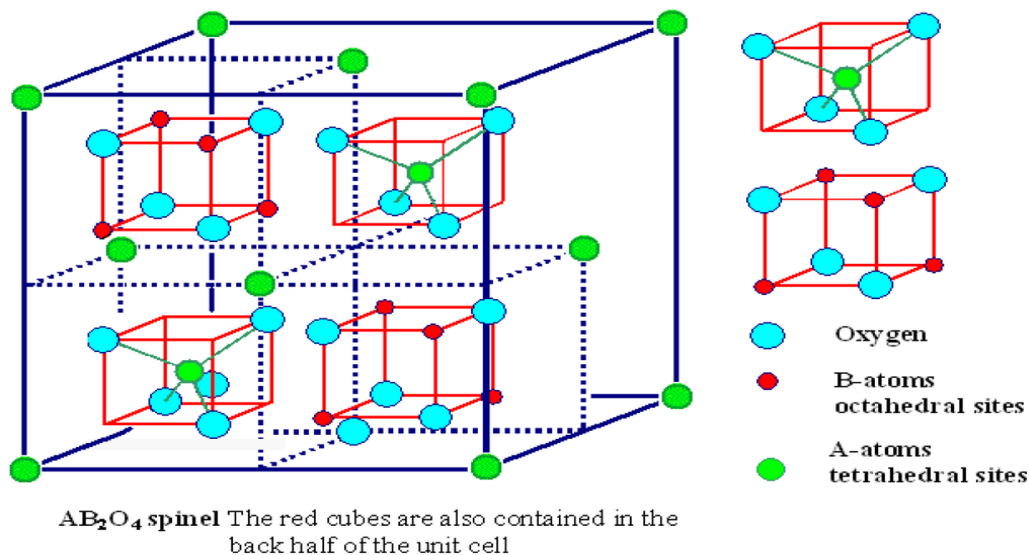


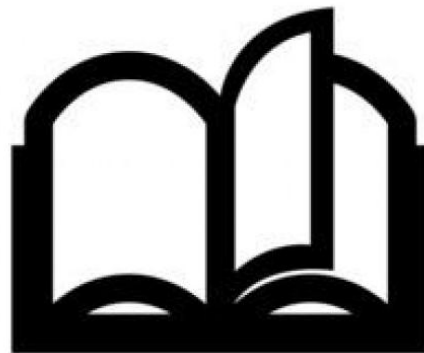
**Fig 1: Unit cell of Mn-Zn Ferrite**

In a spinel structure, both divalent and trivalent cations are distributed among tetrahedral (A) and octahedral (B) sites. The site preference exhibited by divalent ions defines whether the spinel is normal, inverse or mixed. In normal spinel, the A<sup>2+</sup> ions occupy only tetrahedral sites and the B<sup>3+</sup> ions occupy only octahedral sites. In inverse spinel, all the A<sup>2+</sup> ions and half the B<sup>3+</sup> ions sit on the octahedral sites; the tetrahedral sites are occupied now by the other half of the B<sup>3+</sup> ions. In most cases, magnetic divalent cations such as Mn<sup>2+</sup> preferred at octahedral sites and produce an inverse spinel structure. Diamagnetic divalent cations (such as Zn<sup>2+</sup>, Cd<sup>2+</sup>) have preference for the tetrahedral positions and the resulting structure is a normal spinel.

Addition of a non-magnetic ion such as Zn to a spinel ferrite leads to an increase in saturation magnetization. Mn-Zn ferrite is a normal spinel, indicating that Zn ions have a preference for the A sites, so that on substituting zinc for manganese the occupancy becomes (Fe<sup>3+</sup><sub>1-α</sub>Zn<sup>2+</sup><sub>α</sub>) (Fe<sup>3+</sup><sub>1+α</sub>Mn<sup>2+</sup><sub>1-α</sub>) O<sub>4</sub> in which the first and second brackets indicate occupancy of the A and B sub-lattices respectively. Thus the antiparallel coupling between moments on A and B sites is reduced because the occupancy of A sites by magnetic ions is reduced, and as a consequence the Curie point is lowered. However, the excess of moments on octahedral sites over those on tetrahedral sites is increased so that the magnetization is increased.

## **CHAPTER 2**

# **LITERATURE REVIEW**



## LITERATURE REVIEW

Spinel ferrites of different compositions have been studied and used for a long time to get useful products. Since the research on ferrites is vast and is difficult to collect all the experimental results and information about all types of ferrites in every aspect. Manganese ferrites has been the subject of intensive experimental and theoretical investigation. Dependence of magnetic performance microstructure and local composition of Mn-Zn ferrites prepared by different techniques. All the processes affect the microstructure and initial permeability of Mn-Zn ferrite. In general sintered high frequency ferrites contain pores around a few percent. In order to minimize the porosity and thus enhance the density obtain a high permeability and high density ferrite, the hot pressing technique has been introduced. High density ferrites is prepared by solid state reaction. The pellets made in this method is sintered at 1000<sup>0</sup>C for 24 hrs both in nitrogen and air are produced having 98% of theoretical density. The high density Mn-Zn ferrite attained room temperature saturation magnetization  $M_s = 55.85 \text{ emu/g}$  at 5.4 KOe.

Among the various compositions of Mn-Zn ferrites  $\text{Mn}_{0.6}\text{Zn}_{0.4}\text{Fe}_2\text{O}_4$  ferrite shows a better combination of electrical and magnetic properties. Further Pannaparayil in 1991 showed the usefulness of Mn-Zn ferrites in electrical and electronics induction, especially in high frequency applications up to 10 MHz. It is also reported that magnetization is reduced due to disorder at high temperature for which complex properties arise. The modern trend in ferrites involves the study of disordered magnetic phases as reported by Dorman.

The magnetic susceptibility of ferrite system is studied by Mazhar-ur-Rana using a mutual inductance techniques in the temperatures range of 255 to 600 K. At temperatures above 450 K, the susceptibility follows a Curie Weiss behaviours with negative Curie temperature and below 450 K show marked deviation from Curie law. Also the resistivity at room temperature decreases with increased substitution of  $\text{Zn}^{+2}$  ions. SEM results indicate that sintered ferrites are granular, polycrystalline containing voids. The increase in concentration of manganese favours the formation of Mn-Zn ferrites with lesser voids, larger grains, higher density and hardness of the bulk materials.

Also the magnetic properties and grain boundary structure of Mn-Zn ferrites with the addition of  $\text{Nb}_2\text{O}_5$  is studied by Inaba in year 1994. X-Ray diffraction study of the cation distribution in the Mn-Zn ferrites is also carried out by Abbas. According to them, study of the structure of a spinel should involve the determination of the lattice parameters, the

oxygen positional parameters, and the cation distribution among the tetrahedral and octahedral sites of the anion clos-packed lattice.

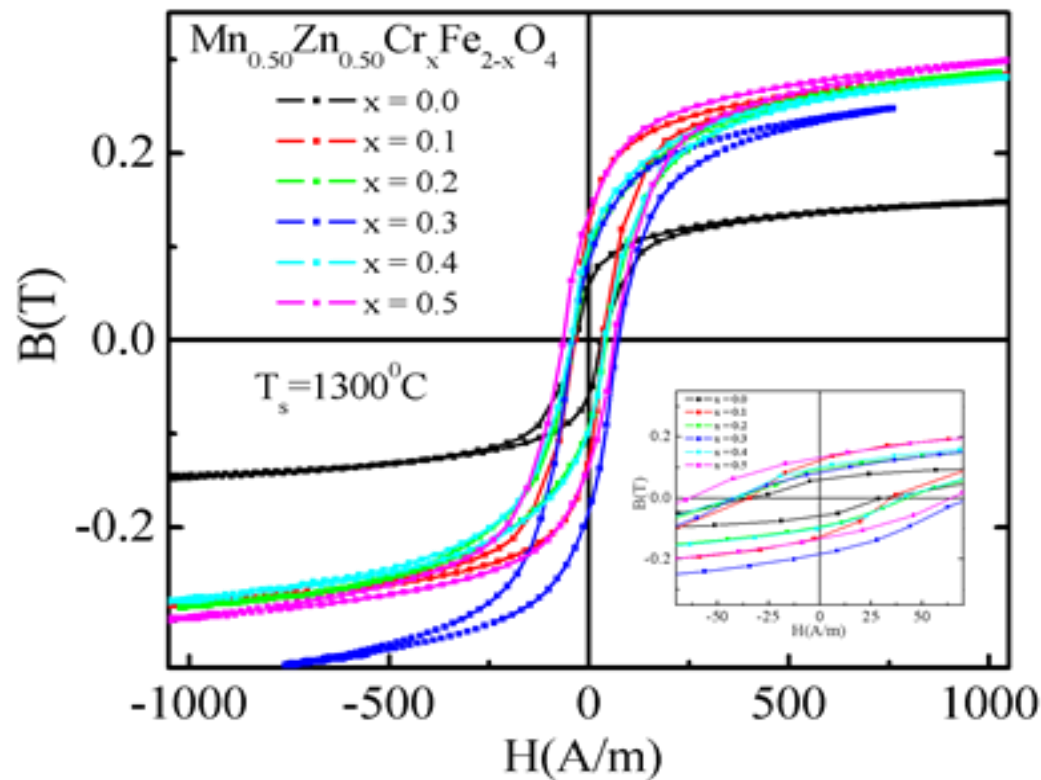


**Fig 2 : B-H loop of Mn Zn Fe<sub>2</sub>O<sub>4</sub>**

Mn ferrites has the highest saturation magnetic moment of any of the simple ferrite Mn-Zn ferrite is a good soft magnetic core material in this sense, but it is not very suitable for extremely high frequency purposes because of its relatively low resistivity. Electrical

transport properties of Zn substituted Mn ferrite has been studied by Ravinder and Reddy. The properties like electrical resistivity, permeability is further improved by adding small amount of Lithium Borosilicate glass. J. Nie studied the effect of nano-sized silica on the power loss properties of the Mn-Zn ferrites and showed that the magnetic properties of low loss Mn-Zn ferrites are greatly dependent upon the amount of nano-SiO<sub>2</sub>. 50 ppm is the optimum content of the nano-SiO<sub>2</sub> to produce uniform grain structure and lowest magnetic loss. Si atoms are enriched in grain boundaries to prevent Ca and Nb atoms from being incorporated within the spinel lattice, so that a high resistivity layer to lower the power loss can be formed. Recently Verma et al. [20] developed a new soft ferrite core for power application. They exploited the best properties of both NiZn and Mn Zn ferrites and developed the Manganese-nickel-zinc ferrite material of Mn<sub>0.2</sub>Ni<sub>0.3</sub>Zn<sub>0.5</sub>Fe<sub>2</sub>O<sub>4</sub> composition. The properties of the developed material suited the applications in switch mode power supplies. The power loss of 500 mw/cc was obtained at a frequency of 500 KHz and a driving flux density of 50 mT in cores of small dimensions.

Amongst the soft ferrites, Manganese Zinc Ferrites are most common, and are used in many more applications than their counterparts, such as nickel-zinc ferrites. Within the Mn-Zn category, large varieties of materials are possible, and the material selection is mainly a function of the application that needs to be accommodated..[3,4]

## OBJECTIVE

- 1) To study the structural and magnetic properties of Mn Zn Ferrite by varying the composition of ZnO and at temperatures 1225 °C, 1250 °C, 1275 °C and 1300 °C.
- 2) To study the variation in density at different temperature.
- 3) To analyse the phase of Mn Zn Ferrite by X-Ray Diffraction.
- 4) To study the Hysteresis loop of Mn Zn Ferrite at different temperature and composition.

## **CHAPTER 3**

# **EXPERIMENTAL PROCEDURE**





## 3.2 SOLID OXIDE MIXING METHOD FOR THE PREPARATION OF Mn-Zn Fe<sub>2</sub>O<sub>4</sub>:

### 3.2.1 MIXING:

Manganese Oxide (MnO) having more than 97% purity, Zinc Oxide (ZnO) are weighed along with the Iron oxide (Fe<sub>2</sub>O<sub>3</sub>) of 98% purity in the fixed proportion of the chemical formula Mn<sub>0.9</sub>Zn<sub>0.1</sub>Fe<sub>2</sub>O<sub>4</sub>, Mn<sub>0.8</sub>Zn<sub>0.2</sub>Fe<sub>2</sub>O<sub>4</sub> , and Mn<sub>0.7</sub>Zn<sub>0.3</sub>Fe<sub>2</sub>O<sub>4</sub> .The weighed raw materials are mixed together thoroughly to get the homogeneous mixture . 0.1weight%, 0.2weight%, 0.3weight% of ZnO to the Bottle 1, Bottle 2, Bottle 3 respectively. Then propanol was added in each jar for mixing because propanol do not react with the composition taken. If water or any other solution were used instead of propanol, that might react with the composition and may change the chemical properties of the composition. After adding iso-propanol to the all 3 compositions, shaken and all the composition powder were wet with the help of iso-propanol. And after that around 30 balls each were put inside all the 3 compositions and then mixing process was carried out by pot milling for 48 hours. And then after 48 hours of homogenisation process, composition paste is taken in the Petridis and left for drying first in the air and the under the IR lamp. This whole process was carried for all the 3 composition with different ZnO percentage. [6]

For the comparison of properties with the addition of different amount of ZnO, 3 compositions were made.

**Table: 1 Amount of different composition taken in grams.**

Composition	MnO <sub>2</sub>	ZnO	Fe <sub>2</sub> O <sub>3</sub>
1	50.625	5.266	103.3187
2	44.826	10.492	102.919
3	39.0464	15.667	102.4564

After pot milling by addition of propanol in the 3 different compositions of powder for 48 hours, the paste was dried under the air and then under the IR lamp.

### **3.2.2 CALCINATION:**

All the three samples with varying additive amount were calcined at 1000 °C for 2 hr, in Electic Arc furnace in air atmosphere. Then the calcined powder were milled by adding acetone with the help of agate mortar to get the fine powder and then again dried the powder under IR lamp.

### **3.2.3 SAMPLE PRPARATIONAND EXPERIMENTATION OF POWDER XRD.**

XRD analysis was carried out to determine the phases present in the composition. X-Ray diffraction was performed with a Philip's Diffractometer (Model: PW-1830, Philips, Netherlands) to obtain the phases present in the calcined powder. After performing the X-Ray diffraction with the Philip's Diffractometer, a graph was plotted between X-Rays intensity against the angle Theta. The angle of each diffraction was converted to d-spacing by using the Bragg's Law i.e.  $n\lambda = 2d \sin\theta$  (where 'n' is the order of diffraction and 'λ' is the wavelength of X-ray. For the identification of different phases present in the calcined powder, Philips X-pert high score software was used.

### **3.2.4 FORMING**

After calcination of the powder samples and the phase confirmation, calcined powder of all 3 compositions was mixed thoroughly with 2 wt. % of binder i.e. polyvinyl alcohol with the help of agate mortar and pestle. In the starting, calcined powder of each composition were mixed with the PVA binder for approximately 1 hour. The powder mixed with PVA was then dried under the IR lamp. After the drying, nice granules of ferrite powder were produced where that granules having good flow ability and compressibility. After that, the granulated powders were uniaxially pressed at a load of 4.2 US Ton with the dwell time of 90 sec by using a hydraulic press to form a pellet of 10.1 mm diameter. Green density of the green pellet was calculated from weight/volume. From the green pellets, volume was calculated and weight was measured in the starting by using weighing balance. Then the sintering of green samples were performed by firing the pellets in an electric arc furnace at different temperatures.

### 3.2.5 SINTERING

Sintering was carried out in (1) an Electrical furnace (chamber furnace of highest temp.

1400 °C) . The details of firing schedule with sintering temperatures has been given in a table below:

**Table: 2 Firing schedule and sintering temperature**

<b>Sintering</b>	<b>Rate upto binder burnout</b>	<b>Binder burnt-out temperature</b>	<b>Rate up to soaking temperature</b>	<b>Sintering Temperature (°C) With (Soaking temp.)</b>
1	2 <sup>0</sup> C /min	600 °C/2hr	3 <sup>0</sup> C / min	1225/2hr
2	2 <sup>0</sup> C /min	600 °C/2hr	3 <sup>0</sup> C / min	1250/2hr
3	2 <sup>0</sup> C /min	600 °C/2hr	3 <sup>0</sup> C / min	1275/2hr
4	2 <sup>0</sup> C /min	600 °C/2hr	3 <sup>0</sup> C / min	1300/4hr

**3.2.6** A flow chart has been represented to summarize the synthesis work.

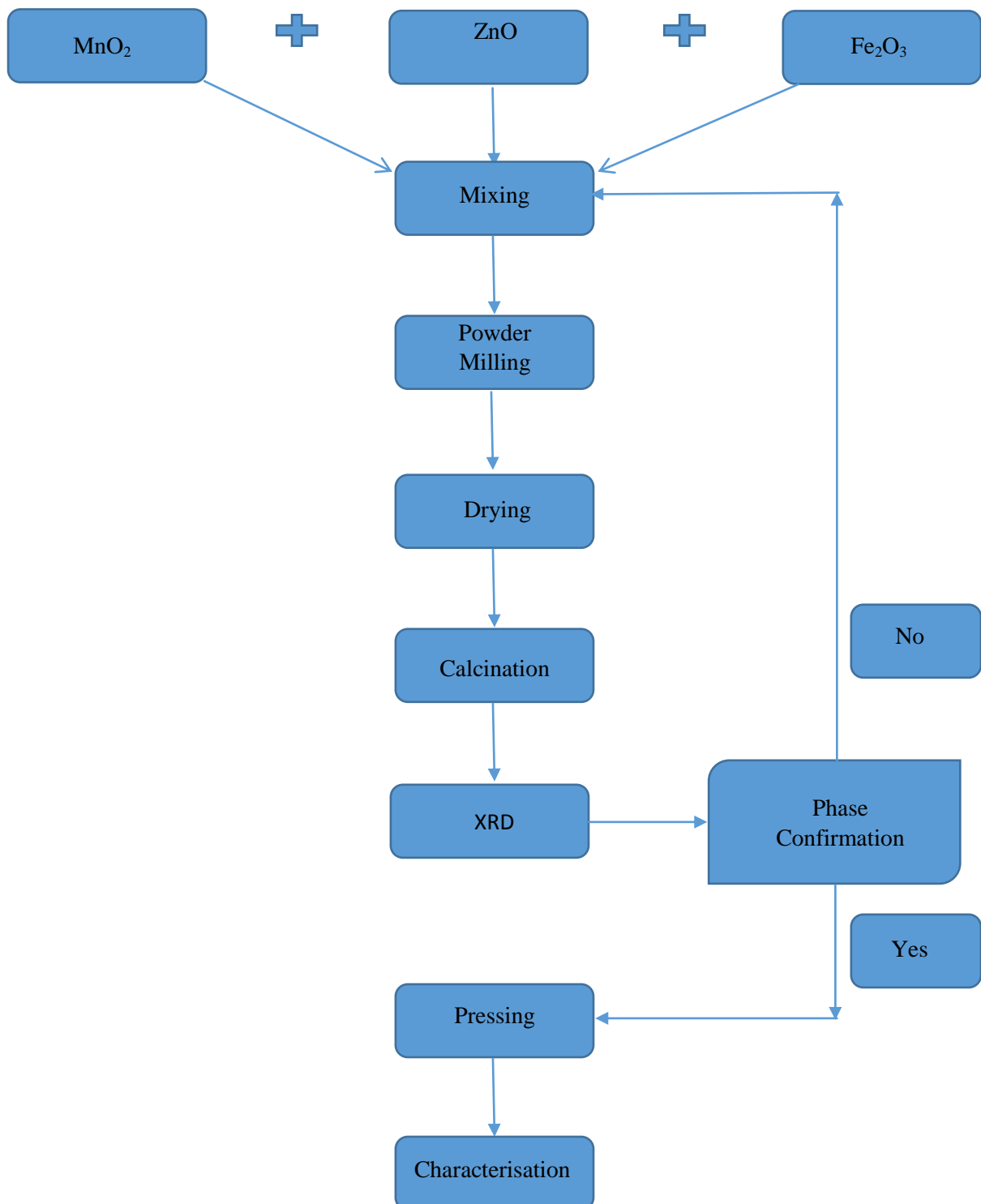


**Fig 3: Flow chart for the synthesis of Manganese Zinc Ferrite.**

### 3.3 Characterization

For the characterisation of sintered pellets, various physical properties of the sintered pellets such as bulk density, apparent porosity, phase analysis, microstructural analysis and magnetic properties such as B-H loop measurement were carried out for all the pellets of all 3 composition.[7]

#### 3.3.1 Phase Analysis by X-Ray Diffraction(XRD):

X-Ray Diffraction was performed with a Philip's Diffractometer (model: PW-1830, Philips, Netherlands). The phase formation in the sintered pellets is studied and the phases present in the sample were identified by using the software called Philip's X-pert high score.

#### 3.3.2 Apparent Porosity and Bulk Density:

Bulk density and apparent porosity of sintered pellets was found out by using the '**Archimedes principle**'. First, measured the dry weight of pellets by using the weighing balance. Then the sintered samples were kept in the beaker containing kerosene and kept in a vacuum chamber so that all the pores were filled up with kerosene completely. Beaker was kept in chamber for about 2 to 3 hours until the bubbling stops in the chamber. After that, Suspended weight and soaked weight of each pellet was measured using the electronic balance.

Apparent porosity and bulk density were calculated by using the formulas given below:

$$\text{Apparent porosity} = \frac{W-D}{W-S}$$

$$\text{Bulk density} = \frac{D}{W-S}$$

Where, D is dry weight.

W is soaked weight.

S is suspended weight.

### **3.3.3 Microstructural Analysis:**

By using Scanning Electron Microscopy (SEM), the microstructure of the sintered pellets were identified. Firstly, before performing the SEM, the pellets were thinly coated by palladium under vacuum condition so as to make the surface conducting for viewing through NOVA NANOSEM 450. The mounted samples were studied by SEM (JEOL- JSM 6480 LV). The Grain size of the pellets is found out by using the “Image J” software.

### **3.3.4 B-H Loop Measurement:**

For the measurement of magnetic property, one “Magneta” Plus field magnetic loop tracer was used. Before performing the measurement, dry weight and the volume of the samples were measured for the calibration. The “applied magnetic fields” were ranging from -4800 to +4800 Oe.

# CHAPTER 4

## RESULTS AND DISCUSSION



## 4.1 X-Ray Diffraction Analysis

### 4.1.[A] X-Ray diffraction analysis of calcined powder

X-ray diffraction experiments were performed with each calcined powder to see the appearance of phase or phases in specimens. The calcined temperature was fixed at 1000 °C for 2hr to obtain phase pure spinel ferrites viz.,  $\text{Mn}_{0.9}\text{Zn}_{0.1}\text{Fe}_2\text{O}_4$ ,  $\text{Mn}_{0.8}\text{Zn}_{0.2}\text{Fe}_2\text{O}_4$  and  $\text{Mn}_{0.7}\text{Zn}_{0.3}\text{Fe}_2\text{O}_4$  as target composition. Their XRD graphs of calcined powders has been represented in Fig. 4.

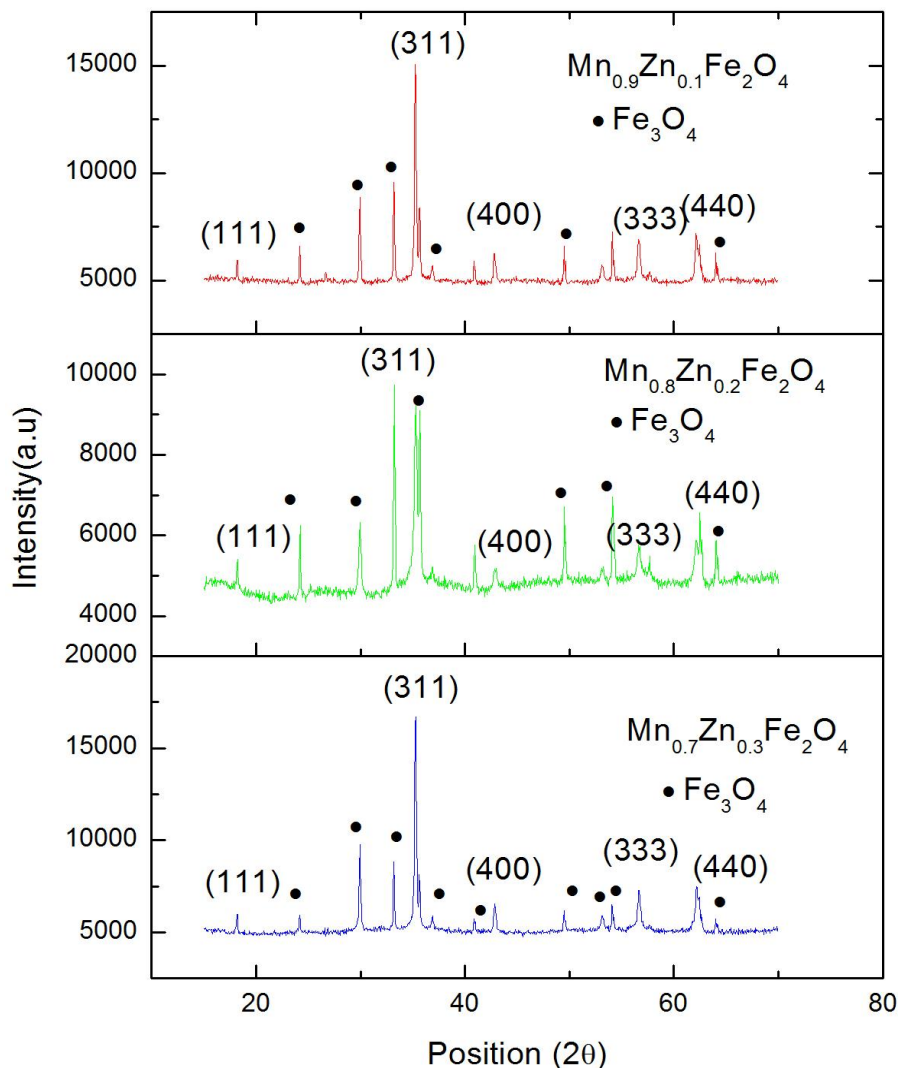


**Fig. 4: XRD pattern of calcined powder(1000 °C/2hr)  $\text{Mn}_{(1-x)}\text{Zn}_x\text{Fe}_2\text{O}_4$ ;  $x = 0.1, 0.2$  and  $0.3$**

The patterns are indexed according to standard procedure of indexing of XRD pattern. The X-Ray diffraction graphs show the peaks with corresponding crystallographic planes. The



obtained pattern is not phase pure as impurity phases are also associated with spinel structure. The peaks due to the impurities were marked by symbol dot. The main impurity was identified as unreacted  $\text{Fe}_2\text{O}_3$ , The main phase  $\text{Mn}_{0.9}\text{Zn}_{0.1}\text{Fe}_2\text{O}_4$ , were obtained matched with a reference pattern from JCPDS (33-0664) database. The following table represents the crystallographic information that include lattice parametres and crystallite sizes.

**Table 3: Crystallite Size of calcined  $\text{Mn}_{(1-x)}\text{Zn}_x\text{Fe}_2\text{O}_4$  powders at 1000 °C, (x= 0.1, 0.2 0.3)**

Composition	Lattice parameter(Å)	Crystallite size (nm)
$\text{Mn}_{0.9}\text{Zn}_{0.1}\text{Fe}_2\text{O}_4$	8.342	37.30
$\text{Mn}_{0.8}\text{Zn}_{0.2}\text{Fe}_2\text{O}_4$	8.346	48.23
$\text{Mn}_{0.7}\text{Zn}_{0.3}\text{Fe}_2\text{O}_4$	8.353	41.34

From the above result it could be state that there is no phase pure  $\text{Mn}_{(1-x)}\text{Zn}_x\text{Fe}_2\text{O}_4$  in case of phase evolution but the  $\text{Mn}_{(1-x)}\text{Zn}_x\text{Fe}_2\text{O}_4$  comes along a small amount  $\text{Fe}_3\text{O}_4$ . That could be due to on reacted  $\text{Fe}_2\text{O}_3$  in powder sample. Regarding lattce parameter, there are apparently no change but a little in increase is been reported. That may be due to replacement with higher ionic size of Zn instead of Mn in basic spinel structure. Crystallite sizes are what have already been reported by some other groups [10].

In order to make practically usable calcined powders have been compacted into pellets and sintered at varying temperature to see the phase stability and density as well. XRD result has been asanalyzed with matching with standard pattern from JCPDS. The result have been discussed with XRD pattern along with lattice parameters and crystallite sizes.

#### 4.1.[B] X-Ray diffraction analysis of sintered pellet:

##### I XRD pattern of pellets sintered at 1225 °C/2hr

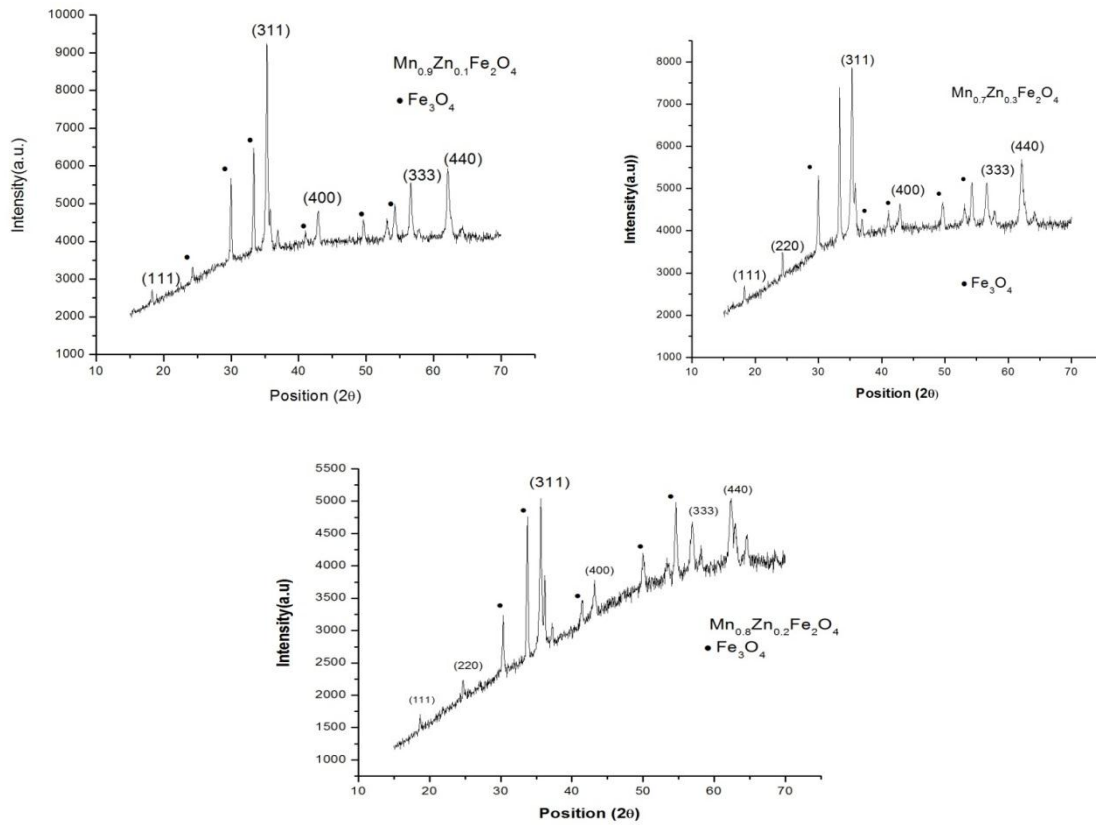
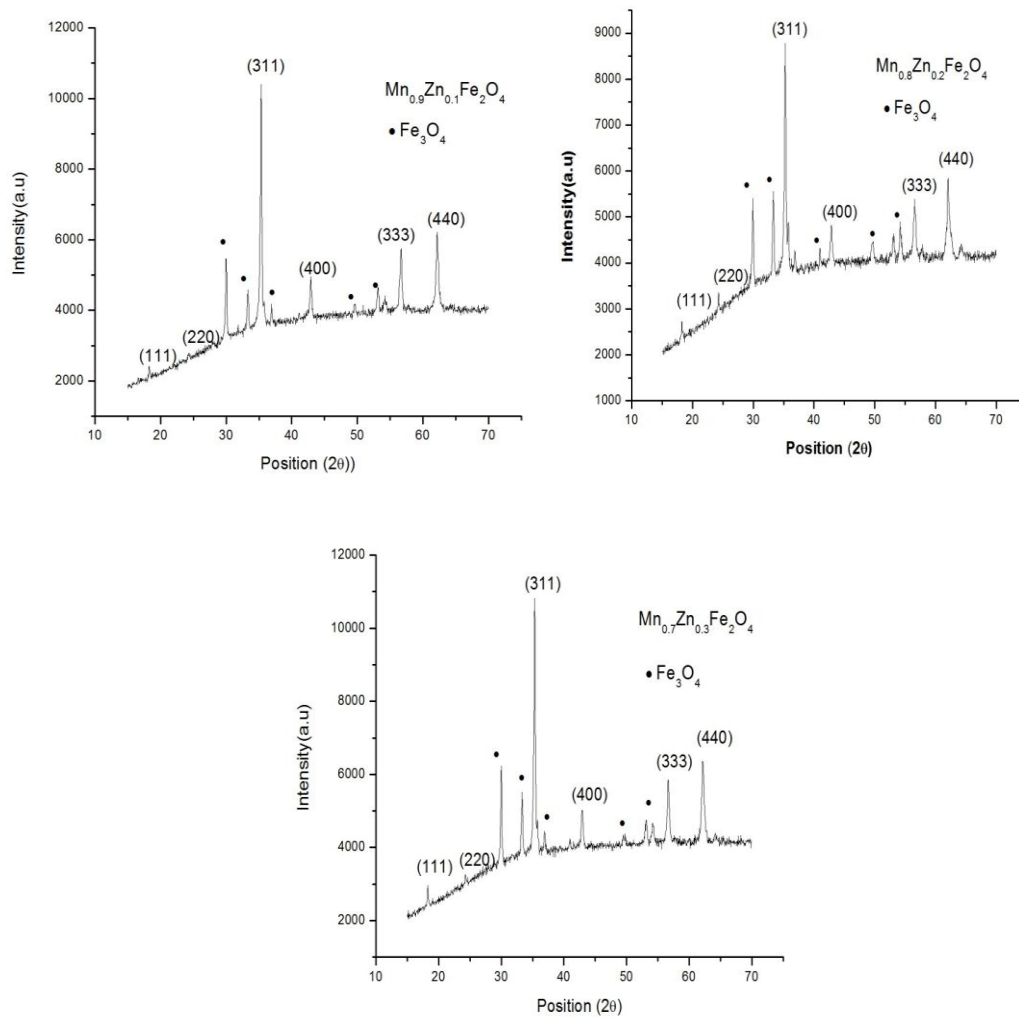


Fig 5: XRD pattern of sintered Mn<sub>(1-x)</sub>Zn<sub>x</sub> ferrite pellets at 1225 °C ,(x=0.1,0.2,0.3)

Table 4: lattice parameter and crystallite size of calcined ferrites Mn<sub>0.9</sub>Zn<sub>0.1</sub>Fe<sub>2</sub>O<sub>4</sub>, Mn<sub>0.8</sub>Zn<sub>0.2</sub>Fe<sub>2</sub>O<sub>4</sub> and Mn<sub>0.7</sub>Zn<sub>0.3</sub>Fe<sub>2</sub>O<sub>4</sub>

Composition	Lattice parameter (Å)	Crystallite size(Å)
Mn <sub>0.9</sub> Zn <sub>0.1</sub> Fe <sub>2</sub> O <sub>4</sub>	8.354	37.3
Mn <sub>0.8</sub> Zn <sub>0.2</sub> Fe <sub>2</sub> O <sub>4</sub>	8.345	30.4
Mn <sub>0.7</sub> Zn <sub>0.3</sub> Fe <sub>2</sub> O <sub>4</sub>	8.347	25.9

## I I XRD pattern of pellets sintered at 1250 °C/2hr



**Fig. 6** XRD plot of Mn-ZnFe<sub>2</sub>O<sub>4</sub> pellets of 0.1 ,0.2 0.3 composition respectively sintered at 1250 °C for 2hr.

**Table 5:** lattice parameter and crystallite size of calcined ferrites Mn<sub>0.9</sub>Zn<sub>0.1</sub>Fe<sub>2</sub>O<sub>4</sub>, Mn<sub>0.8</sub>Zn<sub>0.2</sub>Fe<sub>2</sub>O<sub>4</sub> and Mn<sub>0.7</sub>Zn<sub>0.3</sub>Fe<sub>2</sub>O<sub>4</sub>

Composition	Lattice parameter (Å)	Crystallite size (nm)
Mn <sub>0.9</sub> Zn <sub>0.1</sub> Fe <sub>2</sub> O <sub>4</sub>	8.343	30.3
Mn <sub>0.8</sub> Zn <sub>0.2</sub> Fe <sub>2</sub> O <sub>4</sub>	8.346	33.8
Mn <sub>0.7</sub> Zn <sub>0.3</sub> Fe <sub>2</sub> O <sub>4</sub>	8.355	33.6

### III XRD pattern of pellets sintered at 1275 °C/2hr

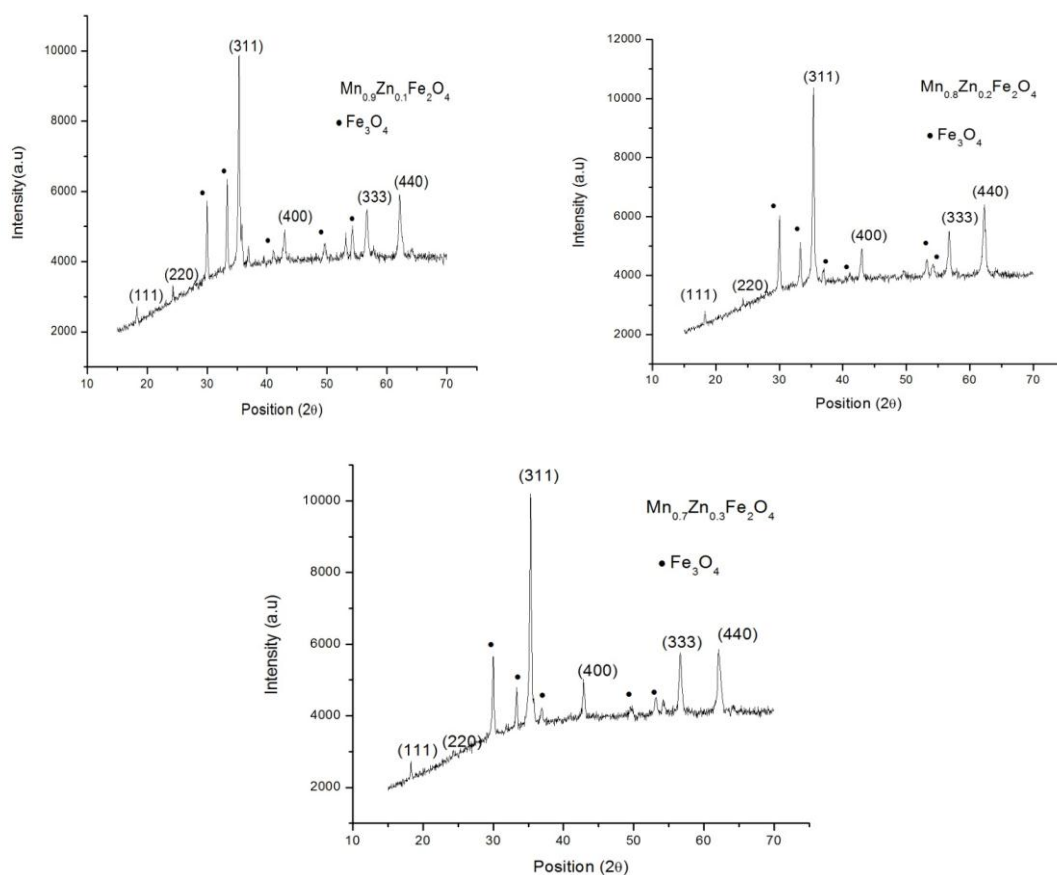


**Fig. 7 XRD plot of Mn-ZnFe<sub>2</sub>O<sub>4</sub> pellets of 0.1 ,0.2 0.3 composition respectively sintered at 1275<sup>0</sup>C for 2hr**

**Table 6 : lattice parameter and crystallite size of calcined ferrites  $\text{Mn}_{0.9}\text{Zn}_{0.1}\text{Fe}_2\text{O}_4$ ,  $\text{Mn}_{0.8}\text{Zn}_{0.2}\text{Fe}_2\text{O}_4$  and  $\text{Mn}_{0.7}\text{Zn}_{0.3}\text{Fe}_2\text{O}_4$**

Composition	Lattice parameter (Å)	Crystallite size (nm)
$\text{Mn}_{0.9}\text{Zn}_{0.1}\text{Fe}_2\text{O}_4$	8.341	34.6
$\text{Mn}_{0.8}\text{Zn}_{0.2}\text{Fe}_2\text{O}_4$	8.352	33.8
$\text{Mn}_{0.7}\text{Zn}_{0.3}\text{Fe}_2\text{O}_4$	8.342	34.6

### III XRD pattern of pellets sintered at 1300 °C/4hr

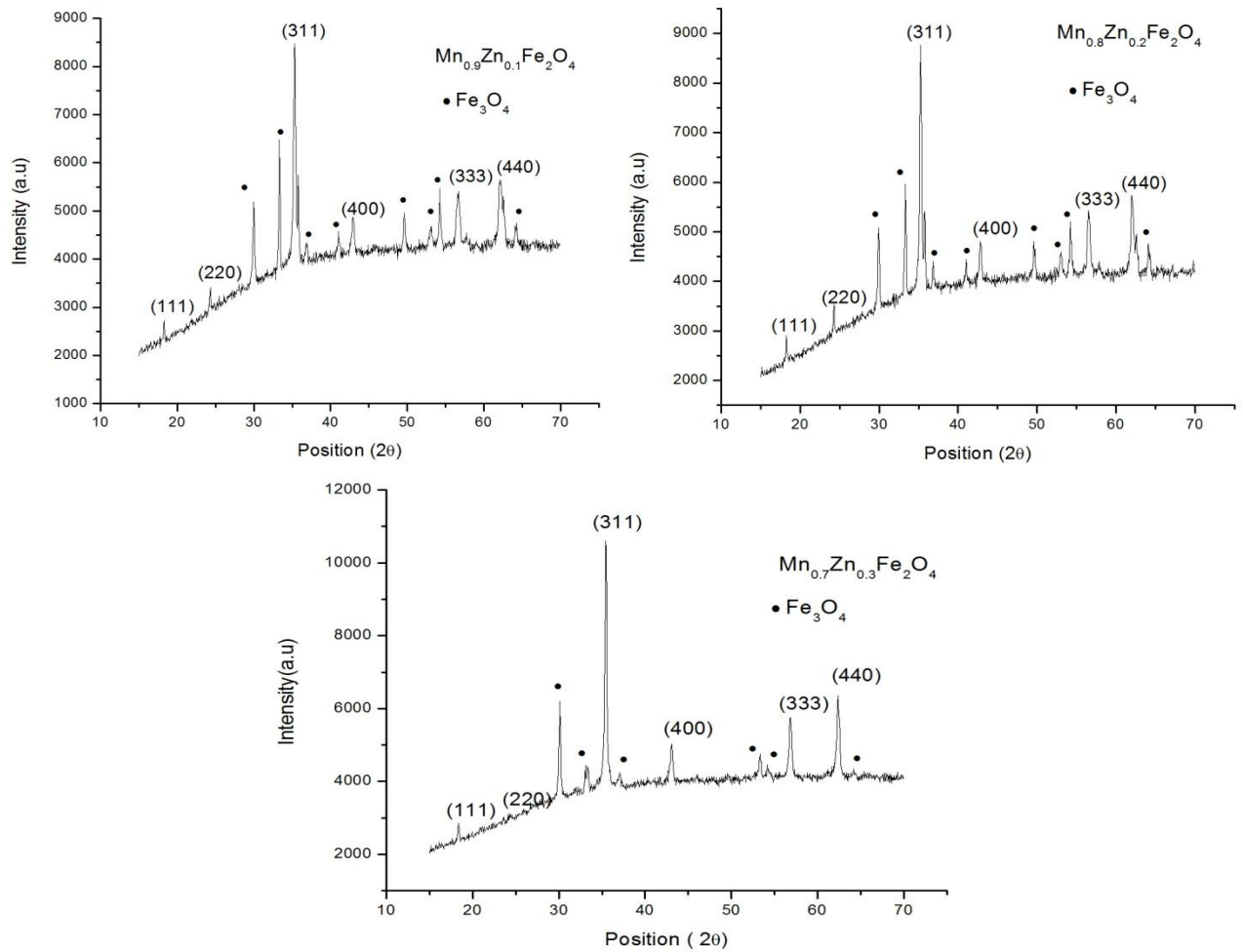


**Fig 8. XRD plot of Mn-Zn  $\text{Fe}_2\text{O}_4$  pellets of 0.1 ,0.2 0.3 composition respectively sintered at 1300 °C for 4hr**

**Table 7 : lattice parameter and crystallite size of calcined ferrites  $\text{Mn}_{0.9}\text{Zn}_{0.1}\text{Fe}_2\text{O}_4$ ,  $\text{Mn}_{0.8}\text{Zn}_{0.2}\text{Fe}_2\text{O}_4$  and  $\text{Mn}_{0.7}\text{Zn}_{0.3}\text{Fe}_2\text{O}_4$  at 1300 °C for 4hr**

Composition	Lattice parameter(Å)	Crystallite size(Å)
$\text{Mn}_{0.9}\text{Zn}_{0.1}\text{Fe}_2\text{O}_4$	8.351	25.9
$\text{Mn}_{0.8}\text{Zn}_{0.2}\text{Fe}_2\text{O}_4$	8.342	36.3
$\text{Mn}_{0.7}\text{Zn}_{0.3}\text{Fe}_2\text{O}_4$	8.356	37.3

Similar study has been made by other two research groups [8,9]

## 4.2 Microstructural Characterization:

Microstructures were analysed with the help of FESEM (Field Emission Scanning Electron Microscopy Technique). The samples were placed under the electron microscope.

I The following figures shows the microstructure of different ferrite composition sintered at 1250<sup>0</sup>C for 2 hours.

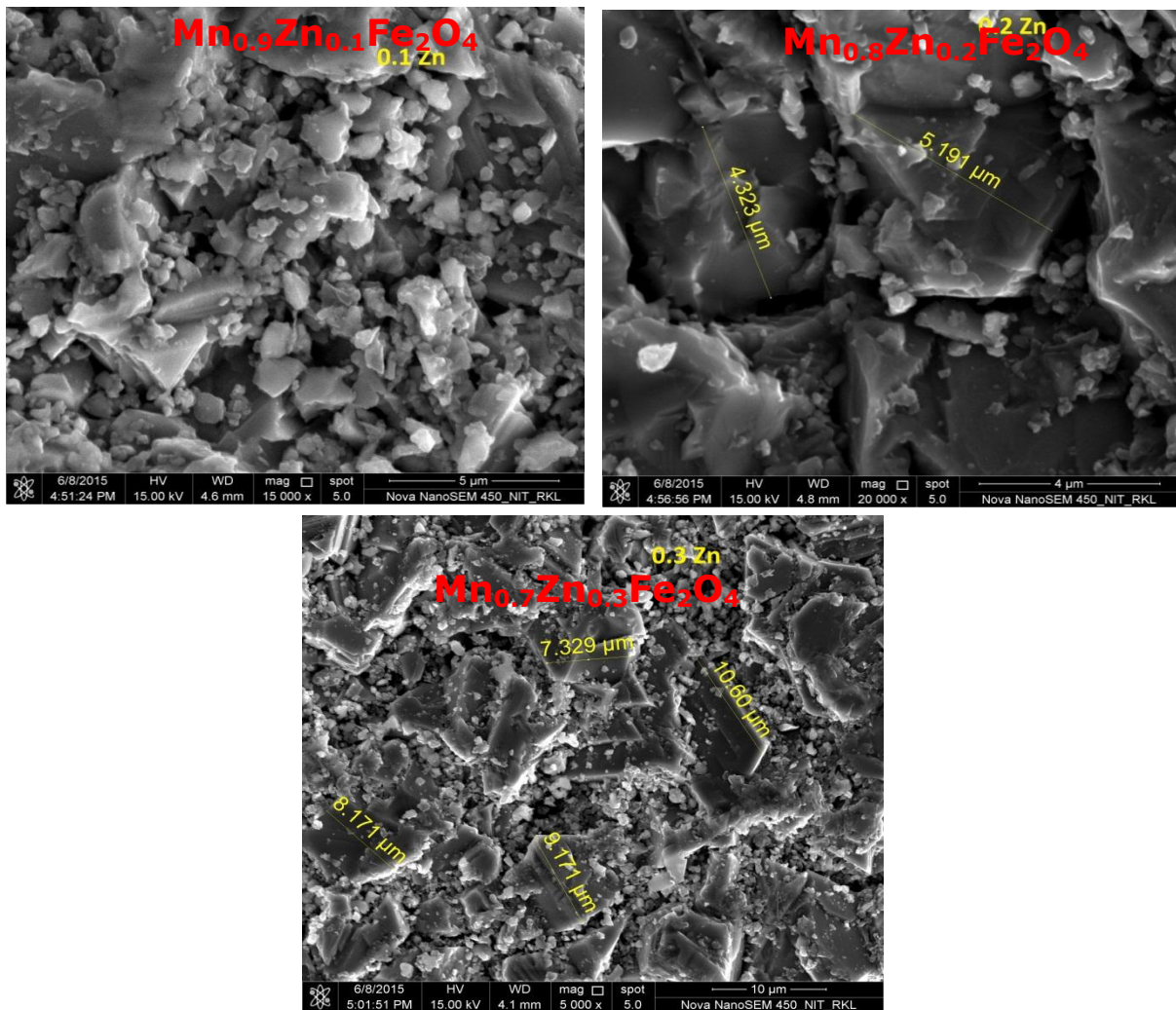


**Fig 9: Microstructures of compositions of  $Mn_{(1-x)}Zn_xFe_2O_4$  sintered at 1250 °C for 2hr**

From figure9, it is very clear that in microstructure various sizes of grain appeared. It may be due to grain growth of a few. Some grains represents well defined *faceted* structure. Sharp boundaries of grains suggest that there is no liquid phase after sintering. The average grain size was calculated with a imaje analysis software and has been represented in following table.



**Table 8 Average grain size of compositions sintered at 1250 °C for 2 hours**

Composition	Grain size range (μm)	Average Grain Size (μm)
$\text{Mn}_{0.9}\text{Zn}_{0.1}\text{Fe}_2\text{O}_4$	0.6-1.5	1.2
$\text{Mn}_{0.8}\text{Zn}_{0.2}\text{Fe}_2\text{O}_4$	0.6-4.7	1.9
$\text{Mn}_{0.7}\text{Zn}_{0.3}\text{Fe}_2\text{O}_4$	0.8-8.8	4.2

**II** The Following figure shows the microstructure of ferrite composition fired at 1275<sup>0</sup>C for 2 hours:

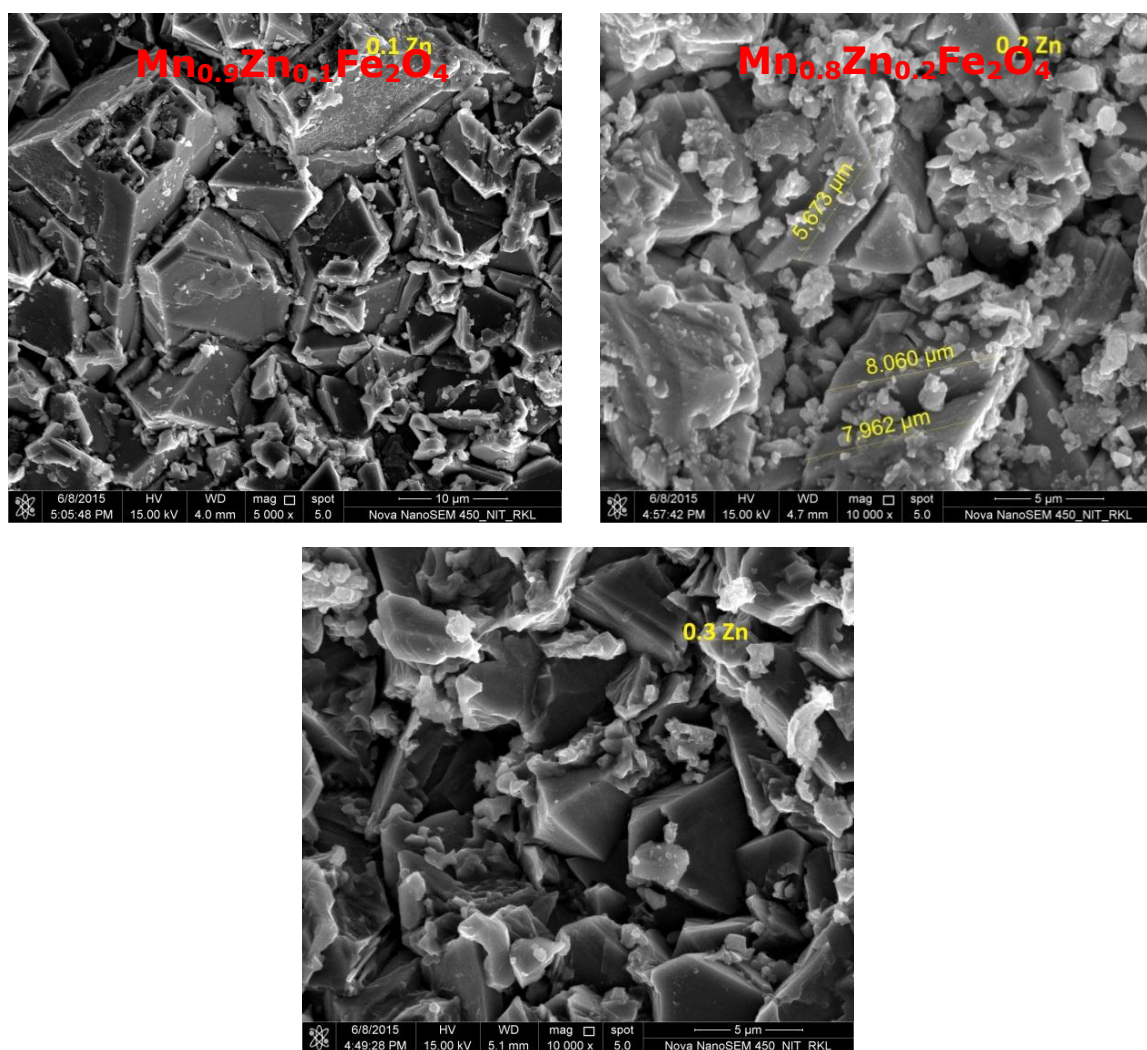


**Fig 10: Microstructures of composition of Mn Zn Fe<sub>2</sub>O<sub>4</sub> sintered at 1275<sup>0</sup>C for 2 hr**

**Table: 9 Average grain size of compositions sintered at 1275 °C for 2 hours**

The Following figure shows the microstructure of ferrite composition fired at 1300 °C for 4 hours.

Composition	Grain Size range (μm)	Average Grain Size (μm)
Mn <sub>0.9</sub> Zn <sub>0.1</sub> Fe <sub>2</sub> O <sub>4</sub>	3.3 – 9.5	6.5
Mn <sub>0.8</sub> Zn <sub>0.2</sub> Fe <sub>2</sub> O <sub>4</sub>	2.5 – 7.5	6.7
Mn <sub>0.7</sub> Zn <sub>0.2</sub> Fe <sub>2</sub> O <sub>4</sub>	2.5 – 7.6	6.2

**III** The following figures shows the microstructure of different ferrite composition sintered at 1300 °C for 2 hours

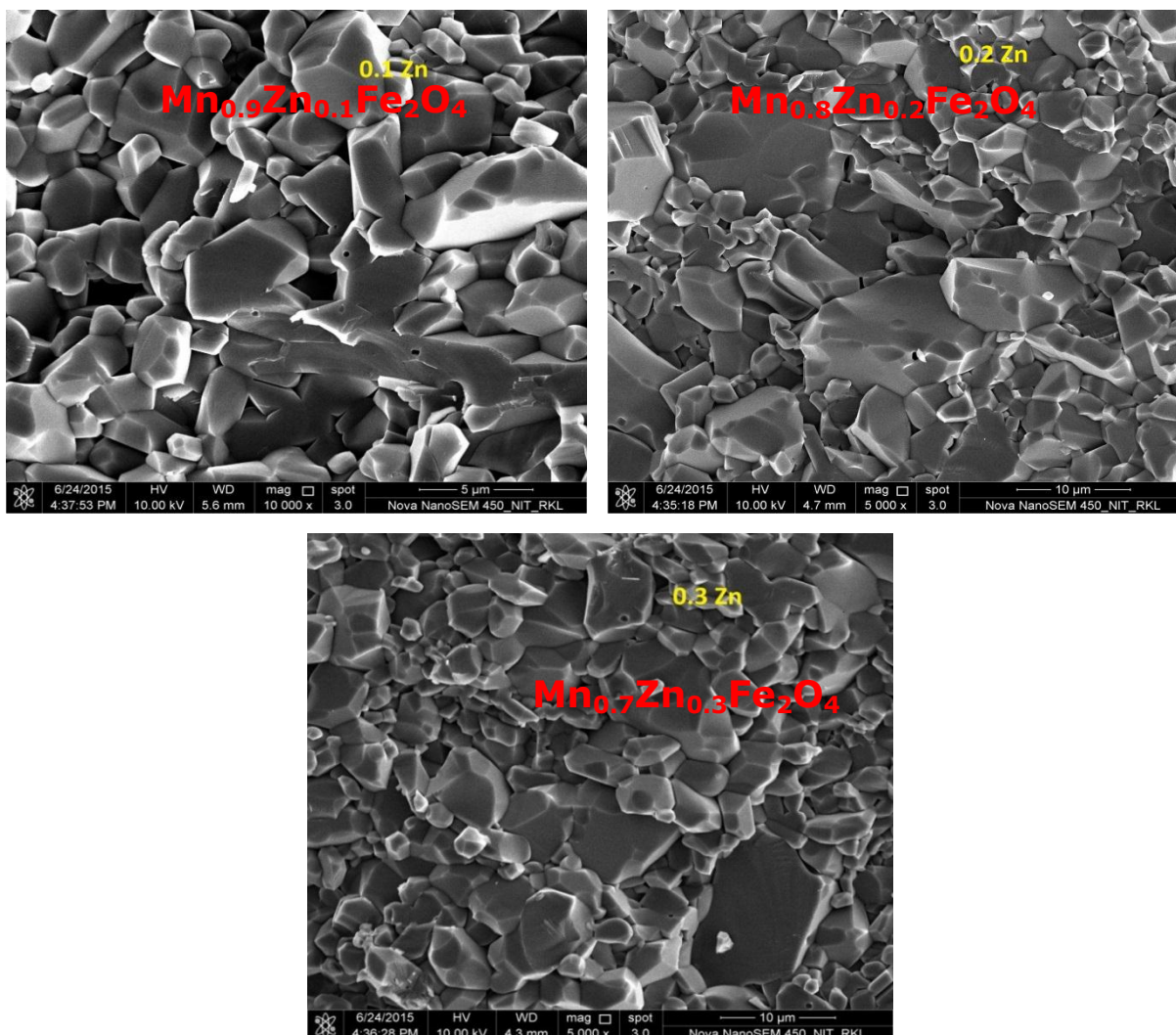


**Fig 11: Microstructures of composition of Mn Zn Fe<sub>2</sub>O<sub>4</sub> sintered at 1275<sup>0</sup>C for 2 hr**

Reference no [10, 11]



**Table 10 Average grain sizes of larger, medium and smaller grain.**

Composition	Grain Size range ( $\mu\text{m}$ )	Average Grain Size ( $\mu\text{m}$ )
$\text{Mn}_{0.9}\text{Zn}_{0.1}\text{Fe}_2\text{O}_4$	1.5 - 6.5	3.9
$\text{Mn}_{0.8}\text{Zn}_{0.2}\text{Fe}_2\text{O}_4$	4.2 – 12.5	8.3
$\text{Mn}_{0.7}\text{Zn}_{0.2}\text{Fe}_2\text{O}_4$	2.4 – 12.2	8.2

Similar works have been represented by more than two research groups [12]

#### 4.3 Bulk Density and Apparent Porosity (B.D. & A.P.)

Bulk density and apparent porosity are important physical property of a ceramic product as those give the idea of other important properties like mechanical strength, magnetic and electrical properties. The table 10 to table 13 shows apparent porosity, bulk density the % densification (of theoretical density) of Mn-Zn Ferrite with varying sintering temperature. for different composition. The tables given below contains the and % of theoretical density of sintered samples. First group of pellets of all three compositions were sintered at 1225 °C. The soaking time for sintering was given as 2 hour.

**Table 11. B.D. and A.P of  $\text{Mn}_{(1-x)}\text{Zn}_x\text{Fe}_2\text{O}_4$  at 1225 °C for 2 hr**

Composition	Bulk Density	Apparent porosity	% of Theoretical Density
$\text{Mn}_{0.9}\text{Zn}_{0.1}\text{Fe}_2\text{O}_4$	4.79	4.3	89.5
$\text{Mn}_{0.8}\text{Zn}_{0.2}\text{Fe}_2\text{O}_4$	4.61	4.8	86.1
$\text{Mn}_{0.7}\text{Zn}_{0.3}\text{Fe}_2\text{O}_4$	4.50	5.1	84.2

As the bulk density value is significantly less as compared to theoretical density of  $\text{Mn}_{(1-x)}\text{Zn}_x\text{Fe}_2\text{O}_4$ . So, the samples of each composition are then sintered at 1250 °C. The soaking time for the sintering is 2 hours.

**Table 12. B.D. and A.P of  $Mn_{(1-x)}Zn_xFe_2O_4$  sintered at 1250 °C for 2 hr**

Composition	Bulk Density	Apparent porosity	% of Theoretical Density
$Mn_{0.9}Zn_{0.1}Fe_2O_4$	4.79	4.3	89.6
$Mn_{0.8}Zn_{0.2}Fe_2O_4$	4.57	4.5	85.4
$Mn_{0.7}Zn_{0.3}Fe_2O_4$	4.72	4.8	88.3

A few samples showed increased B.D. that is why sintering temperature was further increased. Next sintering temperature was chosen as 1275 °C for 2 hour.

**Table 13. B.D. and A.P of  $Mn_{(1-x)}Zn_xFe_2O_4$  sintered at 1275 °C for 2 hour**

Composition	Bulk Density	Apparent porosity	% of Theoretical Density
$Mn_{0.9}Zn_{0.1}Fe_2O_4$	4.85	3.1	90.7
$Mn_{0.8}Zn_{0.2}Fe_2O_4$	4.90	2.9	91.6
$Mn_{0.7}Zn_{0.3}Fe_2O_4$	4.76	3.4	89.1

As represented at table 12, the average B.D value increased significantly. So magnetic characterization of all samples sintered at that temperature were performed.

**Table 14. B.D. and A.P of  $Mn_{(1-x)}Zn_xFe_2O_4$  sintered at 1300 °C for 2 hour**

Composition	Bulk Density	Apparent porosity	% of Theoretical Density
$Mn_{0.9}Zn_{0.1}Fe_2O_4$	4.63	4.3	86.6
$Mn_{0.8}Zn_{0.2}Fe_2O_4$	4.71	4.2	88.1
$Mn_{0.7}Zn_{0.3}Fe_2O_4$	4.68	4.1	87.6

Average value of B.D. of sintered samples (1300 °C/2hour)

From above B.D and A.P data it is clear that, with calcined powder 1275 °C / 2hr as sintering temperature is recommended to obtain optimum density. And similar work has been published by group of people [12,13]

## 4.4 Magnetic characterization

Samples with better B.D. were then taken for measurement in magnetic B-H characteristics as per expectation of better magnetic property. 'Magna' hysteresis loop tracer was employed for seeing the Saturation magnetization, Remnant magnetic and Coercive field.

B-H loop of 0.2 Zn composition at 1275 °C for 2 hours were found as:

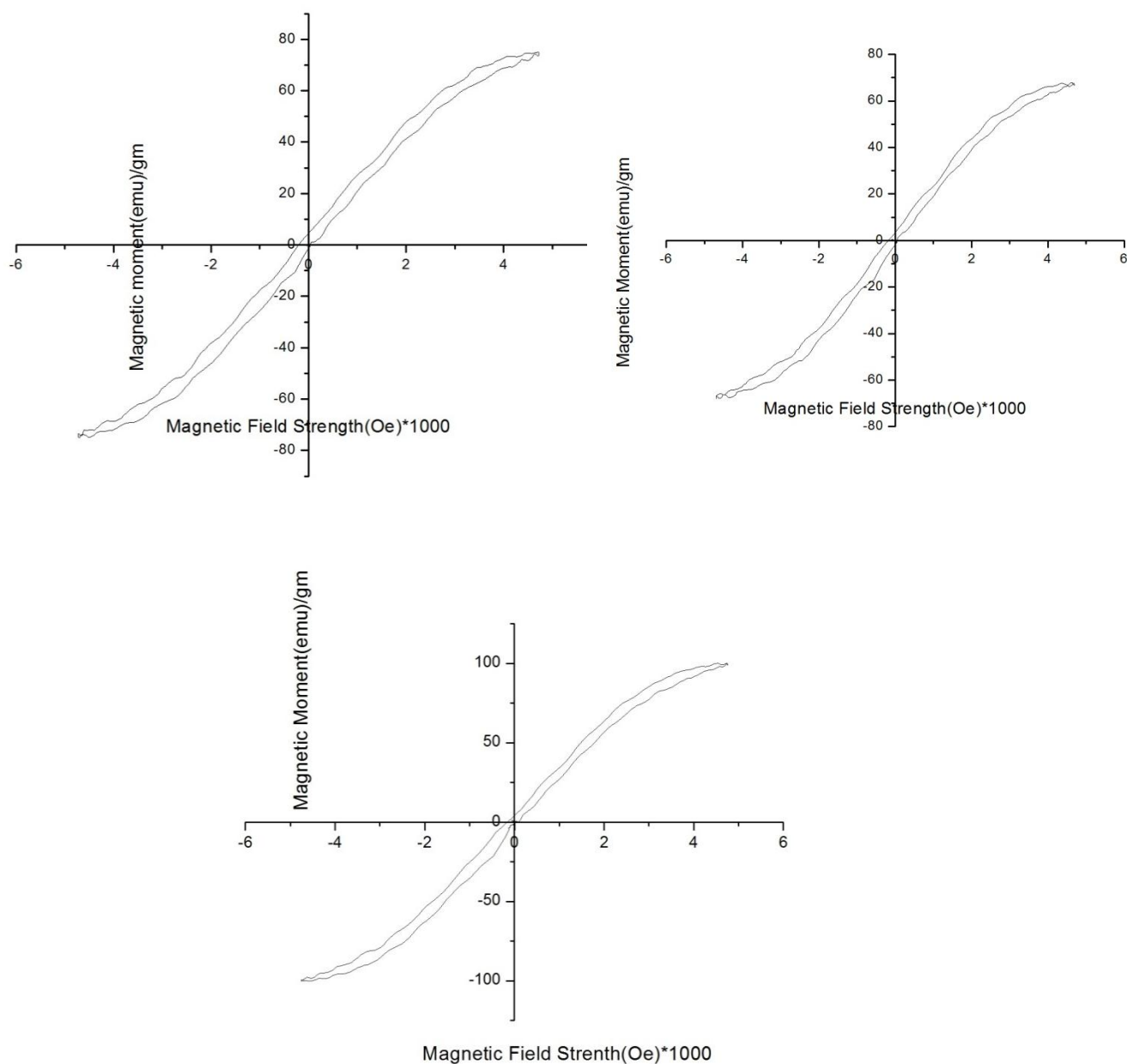


**Fig: 12 B-H loop of Mn Zn Fe<sub>2</sub>O<sub>4</sub> sintered at 1300 °C for 4 hours having 0.2 Zn**

**Table: 15 Magnetic order parameters of  $\text{Mn}_{(1-x)}\text{Zn}_x\text{Fe}_2\text{O}_4$  sintered at 1275 °C/2hr**

<b>Composition</b>	<b>Saturation Magnetization, Ms (emu/g)</b>	<b>Remnant Magnetization, Mr (emu/g)</b>	<b>Coercivity, Hc (Oe)</b>
$\text{Mn}_{0.9}\text{Zn}_{0.1}\text{Fe}_2\text{O}_4$	66.626	6.44	197
$\text{Mn}_{0.8}\text{Zn}_{0.2}\text{Fe}_2\text{O}_4$	74.417	5.914	190
$\text{Mn}_{0.7}\text{Zn}_{0.3}\text{Fe}_2\text{O}_4$	67.098	19.34	240

Similar works have been represented by more than two research groups [14,15]

## **CHAPTER 5**



**CONCLUSION**

## CONCLUSION

- 1)  $\text{Mn}_{(1-x)}\text{Zn}_x\text{Fe}_2\text{O}_4$  powders were synthesised after calcination, where  $\text{Fe}_2\text{O}_3$  remains as impurity.
- 2) Highest obtained Bulk Density of the samples sintered at  $1275^\circ\text{C}/2\text{hr}$  is still less than the bulk density reported by other groups while following same route of synthesis.
- 3) Sintering temperature of  $1275^\circ\text{C}/2\text{hr}$  gave optimal bulk density to all composition.
- 4) Magnetic properties are comparable to typical soft Mn Zn Ferrite sample.
- 5) Pure phase of  $\text{Mn}_{(1-x)}\text{Zn}_x\text{Fe}_2\text{O}_4$  and improved density could lead to enhance magnetic property.

## REFERENCES:

1. K. Praveena, K. Sadhana, S. Bharadwaj, S.R. Murthy, Journal of Magnetism and Magnetic Materials 321 (16) (2009)
2. J. Pankert, Journal of Magnetism and Magnetic Materials 138 (1994) 45.
3. Laishram, R. and Prakash, C. (2006) Journal of Magnetism and Magnetic Materials, 305, 35-39.
4. Praveena, K., Sadhana, K., Bharadwaj, S. and Murthy, S.R. (2009) Journal of Magnetism and Magnetic Materials, 321, 2433-2437.
5. J. Smit and H.P.J. Wijn, in: *Ferrites* (Philips' Technical Library, The Netherlands, 1959) 161.
6. Dasgupta S, Dasb J, Eckertb J, Mannaa I. Influence of environment and grain size on magnetic properties of nanocrystalline Mn–Zn ferrite. J Magn Magn Mater 2006;306:9–15.
7. A. Žnidaršič, M. Ljupel, M. Drofenik, “Effect of Dopants on the Magnetic Properties
8. M. Pardavi-Horvath, “Microwave Applications of Soft Ferrites,” J. Magn. Magn. Mater., 215, 171–83 (2000)
9. Arulmurugan, B. Jeyadevan, G. Vaidyanathan, and S. Sendhilnathan, “Effect of Zinc Substitution on Co–Zn and Mn–Zn Ferrite Nanoparticles Prepared by Co-Precipitation,” J. Magn. Magn. Mater., 288, 470–7 (2005).
10. [1] G. Ott, J. Wrb, R. Lucke, J. Magn. Magn. Mater. 535 (2003) 254–255.
11. M.M. Hessien, M.M. Rashad, K. El-Barawy, I.A. Ibrahim, J. Magn. Magn. Mater. 320 (2008) 1615–1621.
12. J. Kulikowski and A. Lesniewski, J. Magn. Magn. Mat. 19 (1980) 117.
13. P.W. Selwood, in: *Chemisorption and Magnetization* (Academic Press, New York, 1975).
14. J. Smit and H.P.J. Wijn, *Ferrites* (Phillips Technical Library, Eindhoven. The Netherlands. 1959). p. 134.
15. P.J. van der Zaag, J.J.M. Ruigrok, A. Noordermeer, M.H.W.M. van Delden, P.T. Por. M. Th. Reijndt. D.M. Donnet. And J.N. Chapman, J. Appl. Phys. 74.4085 (1993).

